The crystal structure and chemistry of high-aluminium phlogopite

ELISA ALIETTI, MARIA FRANCA BRIGATTI AND LUCIANO POPPI

Dipartimento di Scienze della Terra, Università di Modena, Via S. Eufemia 19, I-41100 Modena, Italy

Abstract

Crystal structure refinements were performed on five Al-rich phlogopite-1*M* crystals ($1.50 \leqslant Al^{3+} \leqslant 1.97$ atoms per formula unit) from skarns of the Predazzo and Monzoni Hills petrographic area (north-east Italy) with the aim of characterizing geometrical variation produced by Al^{3+} increase. The charge imbalance was mostly compensated for by substitutions of highly charged cations in the octahedral sheet (Al^{3+} and/or Fe^{3+} for Mg^{2+}). The refinements were carried out in the mean space group *C2/m* and gave agreement values (*R*) between 0.025 and 0.030. For some additional crystals, only chemistry and/or unit cell parameters were determined. In all samples the tetrahedra are more regular and larger than those previously reported in the literature for phlogopite crystals and the misfit between tetrahedral and octahedral sheets, produced by the increase in the tetrahedral edges, is mostly compensated for by the tetrahedral ring angle rotation α ($10.2° \leqslant \alpha \leqslant 12.5°$), whereas the octahedral sheet features seem affected only by local crystal-chemical variations.

KEYWORDS: Al-rich phlogopite, clintonite, crystal chemistry, structure refinement, skarns.

Introduction

TRIOCTAHEDRAL micas are among the most abundant mafic minerals in the continental crust, where they play major roles in both igneous and metamorphic petrologic processes. However, problems associated with most aspects of their crystallography and crystal chemistry (such as stacking faults, chemical disorder, superstructures, twins and intergrowth with other phases) have prevented its wide use in petrogenetic works.

Aimed at characterizing the crystal-chemical processes occurring in micas, this study affords insight into the structural changes that take place in phlogopite crystals with high Al^{3+} contents ($1.50 \leqslant {}^{[4]}Al^{3+} + {}^{[6]}Al^{3+} \leqslant 1.97$ atoms per formula unit).

Experimental

The phlogopite samples examined in this work were taken from skarns of the Predazzo-Monzoni petrographic area in north-east Italy. Samples 1, 2 and 3 are from Canzoccoli, Predazzo; sample 4 is from Toal de la Foia, Monzoni Hills. Fassaite, vesuvianite, garnet, spinels, forsterite, melilite, epidote, Mg-rich amphiboles, as well as pale green or white micas (clintonite) are the most abundant replacement minerals. Phlogopite commonly occurs with calcite, and sometimes with fassaite and is sometimes closely associated with other micas, such as clintonite. Phlogopite to chlorite alterations at the rim of the grains and along cleavages are sometimes observed (Morandi *et al.*, 1984).

Several crystals selected, after crushing, from the sample rock and examined in the first instance by precession photographs, show that the 1*M* polytype is ubiquitous in the regularly stacked crystals. Some crystals exhibit random stacking indicated by streaks connected with the $k \neq 3n$ spots. Five crystals were selected for further investigation (samples: phl1a, phl1b, phl2a, phl3a, phl4a) since they afforded the most accurate possible X-ray diffraction data. For some additional crystals, only the chemical data and the unit cell parameters have been reported.

Electron probe microanalyses (EPMA) were carried out with an ARL-SEMQ electron microprobe on the same crystal later used for structure refinement. Operating conditions were: accelerating voltage, 15 keV; sample current, 20 nA; beam diameter, 3 μm. Within the expected bounds of

Mineralogical Magazine, March 1995, Vol. 59, pp. 149–157

analytical error, the crystals are homogeneous and their mean compositions are reported in Table 1. Semi-quantitative scanning for all elements with Z > 8 did not clearly reveal the presence of any other elements, although some may exist in undetectable trace amounts. The OH and Fe^{2+} were determined over a wide range of selected crystals, OH by thermogravimetric analysis (Seiko 5200 thermal analyser, heating rate 10°/min in argon gas to prevent iron oxidation) and Fe^{2+} by the semi-micro volumetric method (Meyrowitz, 1970). Structural formulae were calculated on the basis of (O+OH+F) = 12.

Unit-cell dimensions were determined with a CAD4 (Enraf-Nonius) four-circle diffractometer with graphite monochromated Mo-$K\alpha$ X-radiation (λ = 0.7107 Å) by 25 intense reflections ($\theta \geqslant 15°$) which were used in centering each crystal. Least-squares refinement of the setting angles gave the unit cell parameters in Table 2 and the orientation matrix used for data collection. For each crystal the intensity data for the half sphere of reciprocal space $\pm h \pm k + l$ were collected in the θ range, 1.5–35°. On the basis of the $\Delta\omega$–$\Delta\theta$ plot obtained for ten selected reflections, the ω scan mode was selected ($1.5° \leqslant \omega \leqslant 5°$). Three standard reflections were measured to check the stability of the radiation and the crystal orientation. The data were empirically corrected for absorption (using ψ-scan data, North *et al.*, 1968), Lorentz-polarization and background effects. Intensity data of symmetrically-equivalent reflections were averaged and the resulting discrepancy factor (R_{sym}) was calculated (Table 2).

The structure refinements were made by full-matrix least-squares procedure, selecting reflections with $I \geqslant 5\sigma(I)$ and using a version of the program ORFLS (Busing *et al.*, 1962). The initial atomic parameters were taken from Brigatti and Davoli (1990). During the refinements, carried out in the mean space group *C2/m*, fully ionized scattering factors were used for the non-tetrahedral cations, whereas both neutral and ionized scattering factors were used for tetrahedral and anion sites (Brigatti and Davoli, 1990).

Results and discussion

Chemistry

Taking into account the ideal phlogopite composition $[^{[12]}K^{[4]}(Si_3Al)^{[6]}Mg_3O_{10}(OH,F)_2]$, the Al^{3+} for Si^{4+} tetrahedral substitution in the crystals studied is mostly compensated for by the exchange vector, $Si_{-x}Mg_{-y}Al_{x+y}$, where the subscripts x and y refer to the tetrahedral substitution of Al^{3+} for Si^{4+} and the octahedral substitution of Al^{3+} (and/or Fe^{3+}) for Mg^{2+} (and/or Fe^{2+}), respectively. Only in some samples are small amounts of M^{2+} (Ba^{2+} and/or Ca^{2+}) present in the interlayer sites. The limit of Al^{3+} tetrahedral substitution ($Al^{3+} \leqslant 1.50$, Table 1) agrees well with the conclusions of Hewitt and Wones (1975), who stated that in synthetic phlogopites the tetrahedral Al^{3+} content does not exceed 1.65–1.70 atoms p.f.u. Our phlogopite samples are closely associated with clintonite $[^{[12]}Ca^{[4]}(SiAl_3)^{[6]}(Mg_2Al)O_{10}(OH,F)_2]$. Nevertheless, the chemistry of the refined crystals interlayer sites does not seem markedly affected by Ca^{2+} for K^+ substitution. Only in some samples, in which precession photographs reveal lack of regularity in the layer stacking, does this substitution become detectable (cf. sample ph14b, Table 1). This behaviour is probably due to clintonite/phlogopite interlayering. The chemical data obtained from a number of crystals indicate that, in this area, the existence of intermediate terms between clintonite and phlogopite is unlikely. Furthermore, synthetic clintonite crystals also showed a restricted solubility field [from $^{[12]}Ca^{[4]}(Si_{1.6}Al_{2.6})^{[6]}(Mg_{2.6}Al_{0.6})O_{10}(OH,F,Cl)_2$ to $^{[12]}Ca^{[4]}(Si_{1.17}Al_{2.82})^{[6]}(Mg_{2.17}Al_{0.83})O_{10}(OH,F,Cl)_2$; Olesch, 1975].

Structural features

Some refinement data are reported in Table 2. The final atomic parameters are given in Table 3. The calculated bond lengths are listed in Table 4 and some structural parameters derived from structure refinement are shown in Table 5. Table 1 lists the octahedral and interlayer occupancies and the estimated Al^{3+} for Si^{4+} tetrahedral substitution (Alberti and Gottardi, 1988; Brigatti *et al.*, 1991) which has been allocated to each site on the basis of structure determinations and the microprobe analyses. A supplementary table of observed and calculated structure factors is available from the authors on request.

The trends of the isotropic thermal factors ($\beta_{eq.}$) are similar to those previously found for trioctahedral micas (Brigatti and Davoli, 1990; Brigatti *et al.*, 1991; Takeda and Ross, 1975). Of the cation sites, tetrahedral (T) atoms have the lowest values and the interlayer (K) the highest; of the anion sites, the basal tetrahedral oxygen atoms (O1 and O2) have a generally higher $\beta_{eq.}$ than O3 and O4. Nevertheless, comparison with isotropic tetrahedral thermal factors reported for phlogopites and biotites shows that, in our samples, they are generally larger. This observation reflects with an increase in Si/Al tetrahedral disorder (Hazen and Burnham, 1973; Liebau, 1985).

At the end of the structure refinement, the electron density difference map showed maxima which can be attributed to the H^+ position only for samples phl2a

TABLE 1. Chemical data, mean atomic number of octahedral and interlayer sites and Al^{3+} for Si^{4+} tetrahedral substitution as determined by structure refinement (¶) and microprobe analysis for Al-rich phlogopite samples from Predazzo-Monzoni Hills petrographic area

	Phl1a*	Phl1b*	Phl2a*	Phl2b	Phl3a*	Phl3b	Phl3c	Phl4a*	Phl4b	Phl4c
Weight (%)										
SiO_2	38.88	37.68	36.78	37.65	35.27	37.12	39.78	36.95	36.57	37.44
TiO_2	0.41	0.33	0.12	0.09	0.17	0.19	0.22	0.06	0.07	0.04
Al_2O_3	18.17	19.10	19.00	18.95	23.61	18.32	15.45	19.15	20.36	19.19
Fe_2O_3	1.71	1.40	2.78	1.61	2.76	2.30	2.00	2.09	1.58	1.72
FeO	1.94	1.94	0.50	0.50	1.23	1.23	1.23	0.76	0.76	0.76
MgO	23.65	24.30	25.03	25.21	21.11	23.91	25.10	25.12	23.98	24.33
MnO	0.17	0.15	–	0.05	0.59	0.04	0.05	0.12	0.01	0.03
CaO	0.07	–	–	–	0.01	–	–	0.23	1.04	0.39
BaO	–	–	0.53	0.48	0.31	1.55	0.51	0.82	1.26	1.18
Na_2O	0.26	0.27	0.14	0.19	0.12	0.13	0.16	0.11	0.22	0.19
K_2O	10.29	10.29	10.49	10.66	10.56	10.31	10.54	9.99	9.42	9.77
H_2O	4.15	4.15	4.15	4.15	4.10	4.10	4.10	4.30	4.30	4.30
F	0.24	0.38	0.47	0.45	0.16	0.79	0.84	0.27	0.41	0.64
Cl	0.05	–	–	–	–	–	0.01	0.03	–	–
Total	99.99	99.99	99.99	99.99	100.00	99.99	99.99	100.00	99.98	99.98
Structural formulae for (O+OH+F) = 12										
Si	2.74	2.65	2.60	2.65	2.50	2.65	2.81	2.60	2.58	2.64
Al	1.26	1.35	1.40	1.35	1.50	1.35	1.19	1.40	1.42	1.36
Total	4.00	4.00	4.00	4.00	4.00	4.00	4.00	4.00	4.00	4.00
Al	0.24	0.24	0.18	0.22	0.47	0.18	0.09	0.20	0.27	0.23
Fe^{3+}	0.09	0.07	0.15	0.08	0.15	0.13	0.11	0.11	0.08	0.09
Fe^{2+}	0.12	0.11	0.03	0.03	0.07	0.08	0.07	0.04	0.05	0.05
Mg	2.48	2.55	2.63	2.65	2.23	2.54	2.64	2.64	2.52	2.55
Mn	0.01	0.01	–	–	0.04	–	–	0.01	–	–
Ti	0.02	0.02	0.01	–	0.01	0.01	0.01	–	–	
Total	2.96	3.00	3.00	2.98	2.97	2.94	2.92	3.00	2.92	2.92
Na	0.04	0.04	0.02	0.03	0.02	0.02	0.02	0.02	0.03	0.03
K	0.93	0.93	0.95	0.96	0.95	0.94	0.95	0.90	0.85	0.88
Ca	–	–	–	–	–	–	–	0.02	0.08	0.03
Ba	–	–	0.01	0.01	0.01	0.04	0.01	0.02	0.04	0.03
Total	0.97	0.97	0.98	1.00	0.98	1.00	0.98	0.96	1.00	0.97
OH	1.95	1.95	1.96	1.95	1.94	1.95	1.93	2.02	2.02	2.02
F	0.06	0.09	0.11	0.10	0.04	0.18	0.19	0.06	0.09	0.14
O	9.99	9.96	9.93	9.95	10.02	9.87	9.88	9.92	9.89	9.84
Total	12.00	12.00	12.00	12.00	12.00	12.00	12.00	12.00	12.00	12.00
Mean atomic number (e^-)										
M1 Xref	13.2(1)	13.4(1)	13.2(1)		13.3(1)			13.0(1)		
M2 Xref	12.9(1)	12.9(1)	12.9(1)		13.2(1)			12.7(1)		
M1+M2 Xref‡	39.0	39.2	39.0		39.7			38.4		
M1+M2 EPMA†	39.0	39.1	38.8		39.8			38.4		
K Xref	17.6(2)	17.80(4)	19.00(4)		18.9(1)			19.06(4)		
K EPMA	18.1	18.1	18.8		18.8			18.9		
Tetrahedral Al occupancies (%)										
$Al^{[IV]}$¶	32.7	35.0	35.5		36.2			36.3		
$Al^{[IV]}$ EPMA	31.5	33.8	35.0		37.5			35.0		

* crystals used in the structure refinement.

Note: Xref: X-ray refinement; EPMA: electron microprobe; ‡: 2x[(2M(2)+M(1)]; †: sum of octahedral cation electrons; ¶: estimated from structure refinement following the method proposed by Alberti and Gottardi (1988) and adapted to layer silicates (Brigatti *et al.*, 1991); K: interlayer site.

TABLE 2. Selected crystal data and unit cell parameters for Al-rich phlogopite crystals

Samples	Dimensions [mm]	N_{obs}	R_{sym} x 100	R_{obs} x 100	*a* [Å]	*b* [Å]	*c* [Å]	β [°]	*V* [Å^3]
Phl1a*	.33 × .06 × .03	475	2.0	2.9	5.306(1)	9.195(3)	10.272(3)	100.01(2)	493.5
Phl1b*	.18 × .12 × .02	513	2.4	2.8	5.309(2)	9.180(5)	10.291(4)	100.00(4)	493.9
Phl2a*	.27 × .18 × .05	675	2.0	2.9	5.305(2)	9.189(3)	10.286(3)	99.96(2)	493.9
Phl2b	.10 × .10 × .02				5.301(2)	9.187(2)	10.277(2)	99.96(3)	492.9
Phl3a*	.18 × .13 × .04	456	2.0	3.0	5.299(1)	9.179(2)	10.279(3)	99.90(2)	492.5
Phl3b	.12 × .11 × .03				5.310(1)	9.196(3)	10.263(3)	99.94(2)	493.6
Phl4a*	.15 × .12 × .03	464	2.3	2.5	5.307(2)	9.199(1)	10.291(2)	99.89(2)	494.9

Note: $R_{sym} = \frac{\sum_{hkl}\sum_{i=1}^{N}|I_{hkl_i} - I_{hkl}|}{\sum_{hkl}\sum_{i=1}^{N} I_{hkl}}$

* Crystals used for the structure refinements

and phl4a. The OH vector orientation is almost parallel to c* and the O-H separation is 0.92 Å. This behaviour bears out the observations reported by Bailey (1984) for true trioctahedral micas.

The crystal chemical features of Al-rich phlogopites-1*M* are discussed and compared with those of other trioctahedral true micas (phlogopite-1*M* and biotite-1*M* samples) and trioctahedral brittle mica

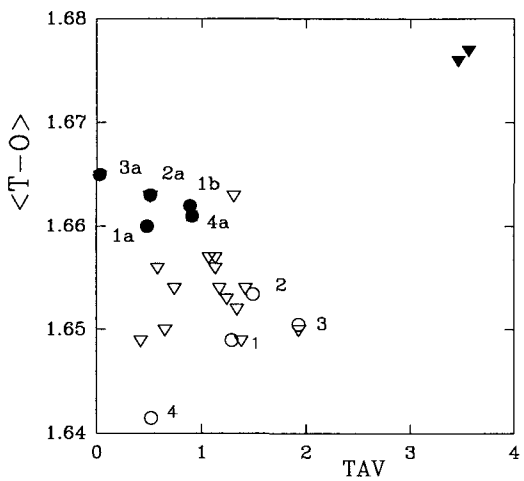

FIG. 1. <T–O> [Å] mean bond lengths *vs* tetrahedral angle variance (TAV). Filled circles: Al-rich phlogopite samples from this study; open circles: phlogopite samples from the literature (1, Hazen and Burnham, 1973; 2, Joswig, 1972; 3, Takeda and Morosin, 1975; 4, McCauley *et al.*, 1973); open triangles: biotite samples from the literature (Brigatti *et al.*, 1991; Brigatti and Davoli, 1990; Bigi and Brigatti, 1994); filled triangles: kinoshitalite (samples 26 and 27 from Brigatti and Poppi, 1993).

kinoshitalite reported in the literature (Fig. 1). These comparisons afford insight into the geometrical variations induced by high Al^{3+}-contents.

Tetrahedral and interlayer sheets. In the 1*M* polytype, the presence of just one symmetrically-independent tetrahedron per unit cell implies no cation ordering. Tetrahedral cation occupancies, as calculated from the structure refinement by the method given in Alberti and Gottardi (1988), are in generally good agreement with those calculated by microprobe analysis (Table 1). The extent of Al^{3+} substitution is always lower than 40%. The tetrahedral mean bond lengths ($1.660 \leqslant <T-O> \leqslant 1.666$ Å; Table 4) are greater than those observed for the Mg^{2+}-true mica end members. The tetrahedra are quite regular ($1.0000 \leqslant TQE \leqslant 1.0002$; $0.03 \leqslant TAV \leqslant 0.91$; TQE and TAV as defined by Robinson *et al.*, 1971) and slightly elongated ($109.6° \leqslant \tau \leqslant 110.3°$; $\tau = 109.47°$ for the ideal tetrahedron) as it is shown in Table 5. In our samples, the increase in tetrahedral Al^{3+} produces more flattened tetrahedra which become more regular (Tables 1 and 5, Fig. 1).

The most significant difference in respect of the crystals of the phlogopite–annite join so far refined is that the tetrahedral ring rotation angle (α) is always higher than 10° (Fig. 2). The α values come near both to those reported for trioctahedral brittle mica kinoshitalite $[^{[12]}Ba^{[4]}(Si_2Al_2)^{[6]}(Mg_3)O_{10}(OH,F)_2]$ (Brigatti and Poppi, 1993) and to dioctahedral muscovite-2M_1 (Bailey, 1984); nevertheless, they are smaller than those found for clintonite-1*M*, where the α values are about 23°. In the trioctahedral subgroup, the tetrahedral Si^{4+} for Al^{3+} substitution in our phlogopite samples is less marked than that observed for kinoshitalite, which has quite similar octahedral compositions (Brigatti and Poppi, 1993). The lateral misfit between tetrahedral and octahedral

TABLE 3. Final atomic positional and equivalent isotropic [A^2] and anisotropic [$A^2 \times 10^4$] thermal factors for Al-rich phlogopite crystals

Atom	x/a	y/b	z/c	$B_{eq.}$	β_{11}*	β_{22}*	β_{33}*	β_{12}*	β_{13}*	β_{23}*
Phl1a										
O1	0.0049(7)	0	0.1716(3)	2.30(8)	255(14)	49(4)	56(3)	0	2(5)	0
O2	0.3333(4)	0.2240(3)	0.1724(2)	2.42(6)	218(9)	74(3)	60(2)	−12(5)	31(4)	−2(2)
O3	0.1308(4)	0.1670(3)	0.3932(2)	1.90(5)	209(9)	38(2)	56(2)	−6(4)	35(3)	2(2)
O4	0.1328(6)	0.5	0.3979(3)	2.63(8)	222(13)	61(4)	81(4)	0	13(5)	0
M2	0	0.3317(2)	0.5	1.55(3)	140(5)	36(1)	48(1)	0	24(2)	0
M1	0	0	0.5	1.58(5)	121(7)	36(2)	56(2)	0	26(3)	0
K	0	0.5	0	3.06(5)	325(8)	92(3)	63(2)	0	31(3)	0
T	0.0767(2)	0.1668(1)	0.2284(1)	1.66(2)	155(3)	40(1)	48(1)	0(2)	22(1)	−1(1)
Phl1b										
O1	0.0029(6)	0	0.1721(3)	2.48(8)	211(11)	76(4)	61(3)	0	9(5)	0
O2	0.3340(4)	0.2228(3)	0.1716(2)	2.43(5)	191(7)	86(3)	58(2)	−21(4)	28(3)	−7(2)
O3	0.1305(3)	0.1669(2)	0.3928(2)	2.02(5)	156(7)	72(3)	48(2)	−4(4)	19(3)	−1(2)
O4	0.1326(5)	0.5	0.3985(3)	2.01(7)	133(10)	70(4)	55(3)	0	20(4)	0
M2	0	0.3316(2)	0.5	1.69(3)	106(4)	55(2)	52(1)	0	20(2)	0
M1	0	0	0.5	1.93(4)	119(6)	63(2)	59(2)	0	22(3)	0
K	0	0.5	0	3.36(5)	284(6)	115(3)	76(2)	0	28(3)	0
T	0.0761(1)	0.1667(1)	0.2287(1)	1.74(2)	115(2)	61(1)	47(1)	−1(2)	17(1)	1(1)
Phl2a										
O1	0.0013(5)	0	0.1718(3)	1.80(6)	188(9)	47(3)	40(2)	0	1(4)	0
O2	0.3358(3)	0.2214(2)	0.1721(2)	1.73(4)	166(6)	57(2)	37(2)	−16(3)	21(2)	−5(2)
O3	0.1313(3)	0.1666(2)	0.3927(2)	1.30(3)	119(5)	40(2)	32(2)	0(3)	15(2)	1(1)
O4	0.1318(4)	0.5	0.3993(2)	1.20(5)	115(8)	33(2)	31(2)	0	9(3)	0
M2	0	0.3308(1)	0.5	1.11(2)	99(3)	27(1)	33(1)	0	13(1)	0
M1	0	0	0.5	1.26(3)	110(5)	34(2)	35(1)	0	12(2)	0
K	0	0.5	0	2.52(3)	251(5)	80(2)	51(1)	0	19(2)	0
T	0.0766(1)	0.1666(1)	0.2284(1)	1.07(1)	96(2)	30(1)	29(1)	−2(1)	10(1)	0(1)
Phl3a										
O1	−0.0064(7)	0	0.1738(4)	2.2(1)	230(15)	52(5)	52(4)	0	−5(6)	0
O2	0.3395(5)	0.2182(3)	0.1732(3)	2.19(7)	214(10)	67(4)	47(3)	−21(5)	10(4)	−5(3)
O3	0.1322(5)	0.1673(3)	0.3937(2)	1.83(6)	205(10)	47(3)	41(2)	4(5)	16(4)	1(3)
O4	0.1306(7)	0.5	0.3997(4)	1.9(1)	161(15)	58(5)	42(4)	0	−10(6)	0
M2	0	0.3309(2)	0.5	1.48(3)	126(5)	40(2)	40(1)	0	1(2)	0
M1	0	0	0.5	1.53(5)	129(8)	39(3)	43(2)	0	2(3)	0
K	0	0.5	0	2.65(5)	263(7)	83(3)	53(2)	0	7(3)	0
T	0.0765(2)	0.1667(1)	0.2285(1)	1.48(2)	137(3)	40(1)	37(1)	−1(2)	2(1)	−2(1)
Phl4a										
O1	0.0031(6)	0	0.1719(3)	2.14(8)	205(12)	41(3)	65(4)	0	5(5)	0
O2	0.3340(4)	0.2225(3)	0.1717(2)	2.20(5)	195(8)	68(3)	52(2)	−20(4)	13(3)	−6(2)
O3	0.1295(3)	0.1670(2)	0.3920(2)	1.57(5)	106(6)	37(2)	56(2)	2(4)	15(3)	4(2)
O4	0.1319(5)	0.5	0.3981(3)	1.55(7)	114(11)	34(3)	54(3)	0	9(5)	0
M2	0	0.3310(2)	0.5	1.42(3)	115(4)	25(1)	53(1)	0	12(2)	0
M1	0	0	0.5	1.62(5)	124(7)	30(2)	60(2)	0	9(3)	0
K	0	0.5	0	2.74(4)	257(6)	78(2)	65(2)	0	12(2)	0
T	0.0764(1)	0.1667(1)	0.2287(1)	1.39(2)	115(3)	25(1)	50(1)	0(2)	8(1)	−1(1)

* $exp[-(h^2\beta_{11} + ... + 2hk\beta_{12} + ...)]$

TABLE 4. Selected bond lengths [Å] for Al-rich phlogopite crystals

	Phl1a	Phl1b	Phl2a	Phl3a	Phl4a
T–O1 [Å]	1.661(2)	1.659(2)	1.662(1)	1.663(2)	1.663(2)
T–O2 [Å]	1.653(2)	1.662(2)	1.660(2)	1.662(3)	1.659(2)
T–O2' [Å]	1.658(3)	1.663(2)	1.664(2)	1.665(3)	1.667(2)
T–O3 [Å]	1.667(2)	1.663(2)	1.665(2)	1.673(3)	1.656(2)
<T–O> [Å]	1.660	1.662	1.663	1.666	1.661
M1–O3 (×4) [Å]	2.076(2)	2.076(2)	2.077(2)	2.075(3)	2.081(2)
M1–O4 (×2) [Å]	2.046(3)	2.047(3)	2.046(2)	2.050(3)	2.053(3)
<M1–O> [Å]	2.066	2.066	2.067	2.067	2.072
M2–O3 (×2) [Å]	2.060(3)	2.061(3)	2.061(2)	2.050(3)	2.061(2)
M2–O3' (×2) [Å]	2.073(2)	2.077(2)	2.073(2)	2.064(2)	2.086(2)
M2–O4 (×2) [Å]	2.061(2)	2.057(2)	2.057(2)	2.048(3)	2.063(2)
<M2–O>[Å]	2.065	2.065	2.064	2.054	2.070
K*–O1 (×2) [Å]	3.409(3)	3.424(3)	3.426(3)	3.470(4)	3.419(3)
K*O1' (×2) [Å]	2.940(3)	2.936(3)	2.927(3)	2.903(4)	2.939(3)
K*–O2 (×4) [Å]	3.408(3)	3.413(3)	3.430(2)	3.464(3)	3.421(2)
K*–O2' (×4) [A]	2.951(3)	2.935(3)	2.927(2)	2.903(3)	2.936(2)
$<K^*–O>_{inner}$ [Å]	2.947	2.935	2.927	2.903	2.937
$<K^*O>_{outer}$ [Å]	3.408	3.417	3.429	3.466	3.420
Delta<K*–O>	0.461	0.482	0.502	0.563	0.483

*K indicate interlayer cation whatever.

sheets in kinoshitalite, which could be produced by the tetrahedral edges increasing, is counterbalanced generally by single polyhedron and tetrahedral ring distortion but in our samples only by tetrahedral ring distortion.

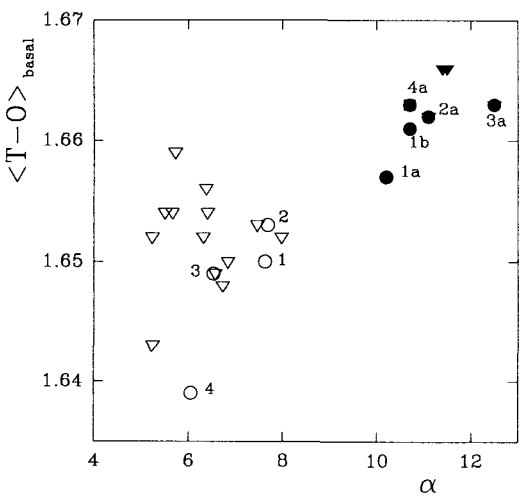

FIG. 2. <T–O> basal [Å] mean bond lengths *vs* the tetrahedral ring rotation angle α[°]. Samples and symbols as in Fig. 1.

Octahedral sheet. The octahedral sites follow the general trend of phlogopite, which is homoctahedral of type I (Weiss *et al.*, 1992), the M1 and M2 mean bond lengths being quite similar within the bounds of experimental error (Table 4). Furthermore, M1 is larger than M2 for sample phl3a, which indicates that the highly-charged cations can be allocated to the M2 site (M1 = $Mg_{0.70}Al_{0.16}Fe^{2+}_{0.07}Mn_{0.04}\square_{0.03}$; M2 = $Mg_{0.76}Al_{0.16}Fe^{3+}_{0.07}Ti_{0.01}$. The cation distribution was hypothesized by structure refinement and using cation radius values calculated by Weiss *et al.*, 1985). <M–O> mean bond lengths are quite similar to those reported in literature for phlogopite and kinoshitalite samples with comparable octahedral chemical composition and thus do not seem markedly affected by tetrahedral sheet dimensions and by tetrahedral ring distortion. The ψ values are all greater than the ideal octahedral value of 54.73°. Both M1 and M2 octahedra show the same flattening, as in phlogopite, with the one exception of sample phl3a, where M1 is more flattened than M2 (Table 5). Figure 3 (*a* and *b*) shows the relationships between the ratio of shared and unshared octahedral edges

TABLE 5. Selected tetrahedral, octahedral and interlayer parameters derived from the structure refinement for Al-rich phlogopite crystals

	Phl1a	Phl1b	Phl2a	Phl3a	Phl4a
Tetrahedral parameters					
α[°]	10.2	10.7	11.1	12.5	10.7
Δz [Å]	0.008	0.005	0.003	0.006	0.002
τ [°]	110.1(1)	110.3(1)	110.1(1)	109.6(1)	110.3(1)
TAV [°]	0.48	0.89	0.51	0.03	0.91
TQE	1.0002	1.0002	1.0001	1.0000	1.0002
$Volume_T$ [Å^3]	2.346	2.355	2.359	2.371	2.352
Octahedral parameters					
ψ_{M1} [°]	58.99	58.92	59.00	59.28	58.75
ψ_{M2} [°]	58.97	58.89	58.93	59.06	58.74
e_{uM1}	3.0663	3.0647	3.0680	3.0763	3.0673
e_{uM2}	3.0637	3.0620	3.0610	3.0517	3.0647
e_{sM1}	2.7690	2.7727	2.7697	2.7597	2.7843
e_{sM2}	2.7680	2.7717	2.7672	2.7505	2.7832
OQE_{M1}	1.0114	1.0110	1.0116	1.0131	1.0103
OQE_{M2}	1.0113	1.0109	1.0114	1.0121	1.0104
OAV_{M1} [°]	37.22	35.95	37.87	42.55	33.67
OAV_{M2} [°]	37.10	35.95	37.42	39.55	34.12
$Volume_{M1}$ [Å^3]	11.561	11.576	11.571	11.542	11.668
$Volume_{M2}$ [Å^3]	11.536	11.556	11.514	11.351	11.644
Sheet thickness [Å]					
tetrahedral	2.253	2.257	2.259	2.250	2.254
octahedral	2.129	2.134	2.130	2.112	2.149
interlayer separation	3.480	3.487	3.484	3.515	3.481

α (tetrahedral rotation angle) = $\sum_{i=1}^{6} \alpha_i/6$ where $\alpha_i = |120°-\phi_i|/2$ and where ϕ_i is the angle between basal edges of neighbouring tetrahedra articulated in the ring;

$\Delta z = [Z_{(O_{basal})_{max}} - Z_{(O_{basal})_{min}}][c\sin\beta]$;

τ (tetrahedral flattening angle) = $\sum_{i=1}^{3}(O_{apical} - T - O_{basal})_i/3$;

TAV (tetrahedral angle variance) = $\sum_{i=1}^{6} (\theta_i - 109.47)^2/5$ (Robinson *et al.*, 1971);

TQE (tetrahedral quadratic elongation) = $\sum_{i=1}^{4} (l_i/l_0)^2/4$ where l_0 is the centre to vertex distance for an undistorted tetrahedron whose volume is equal to that of the distorted tetrahedron with bond length l_i (Robinson *et al.*, 1971);

ψ (octahedral flattening angle) = cos^{-1}[octahedral thickness/(2 <M–O>)] (Donnay *et al.*, 1964);

e_u, e_s: mean lengths of unshared and shared edges, respectively (Toraya, 1981);

OQE (octahedral quadratic elongation) = $\sum_{i=1}^{6}(l_i/l_0)^2/6$ where l_o is the centre to vertex distance for an undistorted octahedron whose volume is equal to that of the distorted octahedron with bond length l_i (Robinson *et al.*, 1971);

OAV (octahedral angle variance) = $\sum_{i=1}^{12} (\theta_i - 90°)^2/11$ (Robinson *et al.*, 1971)

(e_u/e_s) and the octahedral flattening ψ angle for both M1 and M2 sites. The Al-rich phlogopite samples vary widely in the case of the M1 site: between biotites and phlogopites, samples phl4a and phl1b are grouped with biotites, samples phl1a and phl2a are intermediate, whereas sample phl3a is grouped with phlogopite. As regards the M2 site, our samples lie in an intermediate field between biotite and phlogopite.

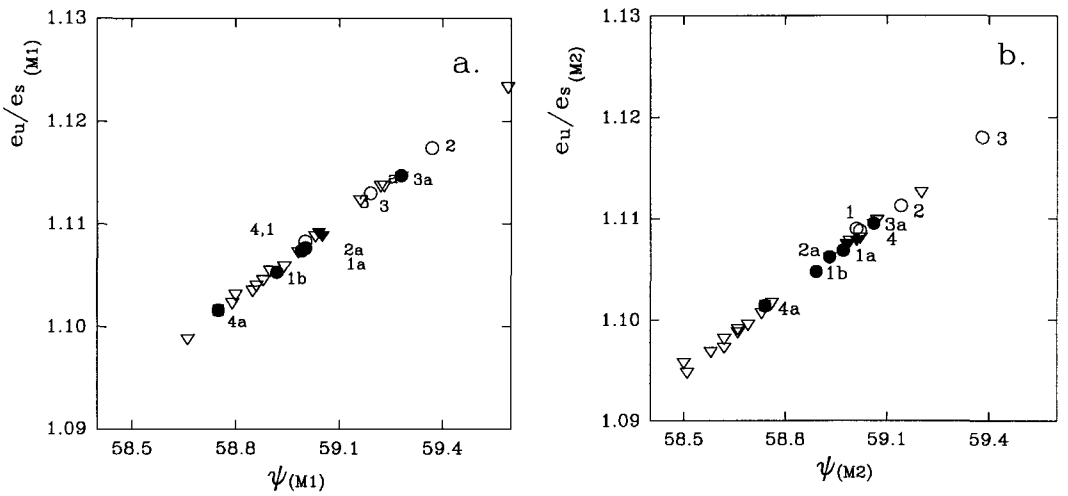

FIG. 3. Variation shown by the ratio of unshared and shared octahedral edges (e_u/e_s) as a function of the octahedral flattening angle (ψ[°]) for Ml (a) and for M2 (b) sites. Samples and symbols as in Fig. 1.

Acknowledgements

We are particularly grateful to C. Nannetti and R. Pirani (Bologna University) for donating the rock samples from Predazzo and Monzoni Hills Petrographic area and to Simona Bigi for technical assistance during electron microprobe determinations. This work was supported by Ministero dell'Università e della Ricerca Scientifica (MURST) and by Consiglio Nazionale delle Ricerche (CNR) of Italy. The Consiglio Nazionale delle Ricerche is also acknowledged for financing the Electron Microprobe Laboratory at Modena University.

References

Alberti, A. and Gottardi, G. (1988) The determination of the Al-content in the tetrahedra of framework silicates. *Zeits. Kristallogr.*, **184**, 49–61.

Bailey, S. W. (1984) Crystal chemistry of the true micas. In *Reviews in Mineralogy* (S. W. Bailey, ed.) Mineralogical Society of America, Washington, **13**, 13–60.

Bigi, S. and Brigatti, M. F. (1994) Crystal chemistry and microstructures of plutonic biotite. *Amer. Mineral.*, **79**, 64–73.

Brigatti, M. F. and Davoli, P. (1990) Crystal-structure refinements of 1*M* plutonic biotites. *Amer. Mineral.*, **75**, 305–13.

Brigatti, M. F., Galli, E. and Poppi, L. (1991) Effect of Ti substitution in biotite-1*M* crystal chemistry. *Amer. Mineral.*, **76**, 1174–83.

Brigatti, M. F. and Poppi, L. (1993) Crystal chemistry of Ba-rich trioctahedral micas-1*M*. *Eur. J. Mineral.*, **5**, 857–71.

Busing, W. R., Martin, K. O. and Levy, H. S. (1962) ORFLS, a Fortran crystallographic least- square program. *U. S. National Technical Information Service*, ORNL-TM-305.

Donnay, G., Donnay, J. D. H. and Takeda, H. (1964) Trioctahedral one-layer micas. II. Prediction of the structure from composition and cell dimensions. *Acta Crystallogr.*, **17**, 1374–81.

Hazen, R. M. and Burnham, C. W. (1973) The crystal structure of one-layer phlogopite and annite. *Amer. Mineral.*, **58**, 889–900.

Hewitt, D. A. and Wones, D. R. (1975) Physical Properties of some synthetic Fe-Mg-Al trioctahedral biotites. *Amer. Mineral.*, **60**, 854–62.

Joswig, W. (1972) Neutronenbeugungsmessungen an einem 1*M*-phlogopit. *Neues Jahrb. Mineral. Mh.*, 1–11.

Liebau, F. (1985) *Structural chemistry of silicates*. Springer, Heidelberg.

McCauley, J. W., Newnham, R. E. and Gibbs, G. V. (1973) Crystal structure analysis of synthetic fluorophlogopite. *Amer. Mineral.*, **58**, 249–54.

Meyrowitz, R. (1970) New semi-microprocedure for determination of ferrous iron in refractory silicate minerals using a sodium metafluoborate decomposition. *Anal. Chem.*, **42**, 1110–13.

Morandi, N., Nannetti, M. C., Pirani, R. and Resmi, U. (1984) La mica verde delle rocce di contatto nell'area Predazzo-Monzoni. *Rend. Soc. It. Min. Petr.*, **39**, 677–93.

North, A. C. T., Phillips, D. C. and Mathews, F. S. (1968) A semi-empirical method of absorption correction. *Acta Crystallogr.*, **A24**, 351–9.

Olesch, M. (1975) Synthesis and solid solubility of trioctahedral brittle micas in the system CaO–MgO–Al_2O_3–SiO_2–H_2O. *Amer. Mineral.*, **60**, 188–9.

Robinson, K., Gibbs, G. V. and Ribbe, P. H. (1971) Quadratic elongation, a quantitative measure of distortion in coordination polyhedra. *Science*, **172**, 567–70.

Takeda, H. and Morosin, B. (1975) Comparison of observed and predicted structural parameters of mica at high temperature. *Acta Crystallogr.*, **B31**, 2444–52.

Takeda, H. and Ross, M. (1975) Mica polytypism: Dissimilarities in the crystal structures of coexisting 1M and $2M_1$ biotite. *Amer. Mineral.*, **60**, 1030–40.

Toraya, H. (1981) Distortions of octahedra and octahedral sheets in 1*M* micas and the relation to their stability. *Zeits. Kristallogr.*, **157**, 173–90.

Weiss, Z., Rieder, M. and Chmielovà, M. (1992) Deformation of coordination polyhedra and their sheets in phyllosilicates. *Eur. J. Mineral.*, **4**, 665–82.

Weiss, Z., Rieder, M., Chmielovà, M., Krajícek (1985) Geometry of the octahedral coordination in micas: a review of refined structures. *Amer. Mineral.*, **70**, 747–57.

[*Manuscript received 15 February 1994: revised 6 July 1994*].